Published in final edited form as:
Biomed Mater. 2020 June 29; 15(4): 045018. doi:10.1088/1748-605X/ab809f.

Transparent support media for high resolution 3D printing of volumetric cell-containing ECM structures

Assaf Shapira[#1], **Nadav Noor**[#1,2], **Hadas Oved**[1], **Tal Dvir**[1,2,3,4,*]

[1]The School for Molecular Cell Biology and Biotechnology, Faculty of Life Sciences, Tel Aviv University, Tel Aviv 6997801, Israel

[2]Department of Materials Science and Engineering, Faculty of Engineering, Tel Aviv University, Tel Aviv 6997801, Israel

[3]The Center for Nanoscience and Nanotechnology, Tel Aviv University, Tel Aviv 6997801, Israel

[4]Sagol Center for Regenerative Biotechnology, Tel Aviv University, Tel Aviv 6997801, Israel

[#] These authors contributed equally to this work.

Abstract

3D bioprinting may revolutionize the field of tissue engineering by allowing fabrication of bio-structures with high degree of complexity, fine architecture and heterogeneous composition. The printing substances in these processes are mostly based on biomaterials and living cells. As such, they generally possess weak mechanical properties and thus must be supported during fabrication in order to prevent the collapse of large, volumetric multi-layered printouts. In this work, we characterize a uniquely formulated media used to support printing of extracellular matrix-based biomaterials. We show that a hybrid material, comprised of calcium-alginate nanoparticles and xanthan gum, presents superb qualities that enable printing at high resolution of down to 10 microns, allowing fabrication of complex constructs and cellular structures. This hybrid also presents an exclusive combination of desirable properties such as biocompatibility, high transparency, stability at a wide range of temperatures and amenability to delicate extraction procedures. Moreover, as fabrication of large, volumetric biological structures may require hours and even days to accomplish, we have demonstrated that the hybrid medium can support prolonged, precise printing for at least 18 hours. All these qualities make it a promising support medium for 3D printing of tissues and organs.

Introduction

Tissue engineering is a multidisciplinary field in which knowledge from medicine, biology and material science is integrated for the purpose of developing bio-artificial alternatives to defected organs. The concept is largely based on fabrication of bio-compatible scaffolds that may be designed to recapitulate the natural extracellular matrix (ECM) of the tissue to be

[*]Correspondence to Tal Dvir (tdvir@tauex.tau.ac.il).

Europe PMC Funders Author Manuscripts

repaired, in terms of its mechanical, topographical and biochemical properties [1–3]. These scaffolds may then be populated with cells that gradually interact and assemble to generate functional tissues in vitro. When adequately matured, these bio-artificial constructs are used to replace or to support the malfunctioning tissue or organ. Nevertheless, the high complexity and fine architecture of living tissues pose a huge challenge, turning their fabrication into an extremely complicated assignment.

The field of 3D bioprinting has evolved rapidly in recent years, allowing to engineer complex and accurate cellularized constructs[4–7]. As opposed to the conventional 3D printing of plastics, ceramics, etc., many restrictions apply when printing delicate biological structures. The printed materials are usually soft, may incorporate living cells (i.e. bioinks), and when extruded onto a hard substrate, might not retain their shape due to weak mechanical properties. This problem is further emphasized when multiple uncured layers of such materials are deposited, one on top of the other, resulting in the collapsing of large volumetric printouts under their own weight[8]. Methods such as co-printing with permanent or sacrificial support materials allow multi-layer printing of bioinks with limited self–supporting capacity and generation of structures that contains overhanging elements. However, to fully circumvent the effect of gravity and to enable the production of volumetric, complex 3D biological structures using very soft materials, new approaches have been developed. Among them are the recently introduced 3D photopatterning and printing in a pre-casted support[5, 9–13].

In 3D photopatterning, the bioink, which contains a photo-responsive crosslinking agent, is pre-casted into a light-transparent container. The latter is then illuminated by a pre-defined pattern to cure a desired structure. Once cured, the structure can be extracted from the bulk for further manipulation[10]. While 3D photopatterning can rapidly produce large and accurate constructs (30–120 seconds for centimeter-scale objects with 0.3 mm features)[9], it lacks the ability to print on-demand various types of cells and materials in different positions, as fabrication is performed on a uniform, pre-casted building substance. This missing quality, though, is important for engineering tissues or organs that are naturally composed of several biomaterials and a heterogenic population of cells.

Printing in a pre-casted support material is another fabrication method. Here, the bioink is extruded through a thin needle into a container filled with a yield stress and shear-thinning support medium which stabilizes the deposited material. To achieve a successful printing, the support medium must allow the needle to move through it easily without interruption, while embracing the printed strand and holding it in position. As long as the bioink and the support media do not intermix, a stable printed pattern can be attained, circumventing the effect of gravity and surface tension. After the completion of the fabrication process and upon curing, the printed construct is extracted by evacuation of the support[5].

This concept was demonstrated by Bhattacharjee *et al* [13]. In this work, the researchers used synthetic, transparent support composed of microscale polyacrylic acid particles for printing complex, volumetric architecture and cell-containing structures. A different technique for the fabrication of such constructs was demonstrated by Jin *et al,* using transparent, Laponite nanoclay support bath [14, 15]. Nevertheless, in both cases, the mechanical force needed for

removal of the support medium, especially from internal voids, may jeopardize the integrity of delicate structures and adversely affect sensitive cells.

A recent innovative work presented the printing of a sacrificial gelatin into a support medium composed of micro-tissues mixed in ECM solution. The gelatin was then sacrificed to leave open vessels within the support that constitutes the parenchyma of the engineered tissue. However, as in 3D photopatterning, this method is constrained by the features of the pre-casted materials and cells. Furthermore, the geometry of the engineered tissue is restricted to the shape of the casting mold[16].

In another study, a semi-transparent support medium composed of gelatin microparticles was developed, allowing high-resolution printing of heart components. In this method, the biomaterial, composed of acid-solubilized collagen, was extruded into the support medium which resulted in its rapid neutralization and curing. An additional, fibrinogen-based bioink was used to introduce cells in between the collagenous shells of the construct. The printout can then be released by quick melting of the support medium upon incubation at 37°C. However, such rapid, thermal release procedure would not suit bioinks that require prolong curing at elevated temperatures. In these conditions, the temperature–sensitive support will start to liquefy before the printout is fully cured, resulting in its distortion[17].

Collagen-based hydrogels are widely used biomaterials that promote cell adhesion, proliferation and differentiation[18]. As opposed to acid-solubilized collagen, the neutral, pepsinized form allows encapsulation of living cells and delicate biofactors, as it remains soluble at cell-friendly pH and gradually cures at body temperature. Recently, our group presented an exclusive form of neutral, pepsinized collagen-based hydrogel (NPCH) which originated from human materials [19, 20]. We then used a uniquely formulated support medium that allowed high-resolution printing of cellular, volumetric, complex bio-structures made of NPCH bioinks or comparable materials[21]. However, emphasis was given to the printed structures and not to the supporting medium.

In this report, we further characterize this transparent, cell-friendly support medium that enables bioink curing at physiological temperature and extraction by a controllable, delicate process. We also provide data on the capacity of this medium to support accurate printing in the microscale, over long time periods, a prerequisite for the printing of detailed, large structures.

Results and Discussion

3D extrusion-based bioprinting is affected by multiple factors that are attributed, among others, to the bioink, the printer and the printing environment. Successful printing could only be achieved following meticulous calibration and fine tuning of key parameters such as the material deposition rate, speed of the printhead, layer height and the geometry of the printed filament. Practically, it is extremely hard to accomplish an optimal balance between these factors without the capacity to visually inspect the process and adjust it while running. Printing in a transparent support medium would thus enable an efficient calibration of these parameters.

To gain both transparency and a wide thermal endurance, we have formulated hydrogel-based support media composed of calcium-alginate particles. To this end, hydrogels were prepared by using the internal gelation technique that is based on slow, uniform release of crosslinking ions pre-mixed with the polymer chains. As opposed to the external gelation method, in which the alginate is non-homogenously crosslinked by diffusion of externally-introduced ions (Figure 1a), the internal gelation process resulted in a highly transparent, homogenous gels (Figure 1b) [22, 23]. The bulk was then grinded and pelleted by centrifugation to yield a particulate medium used to support the printing of NPCH. After curing, the printed construct can be easily extracted by delicate enzymatic degradation or by chelation-mediated dissolution of the support. Interestingly, while optimizing the gel setting and processing procedure, we noticed that supplementing the alginate with an additional soluble polymer may improve both the efficiency of the grinding and the printing supporting features of the resulted preparation. Among the polymers tested, we found that the addition of xanthan gum (XG), a microbial negatively-charged exopolysaccharide, yielded a hybrid support medium with optimal qualities, as will be further discussed (Figure 1c).

Environmental scanning electron microscopy (ESEM) examination of diluted support medium revealed that the latter was composed of alginate nanoparticles (Figure 2a,b). As demonstrated in figures 2c-f, in the presence of XG, the alginate nanoparticles formed significantly smaller aggregates that were homogenously distributed throughout the medium. Rheological measurements showed that a support medium composed only of alginate particles, exhibited a storage modulus of ~100 Pa and a yield stress value of ~30 Pa, comparable to an aqueous solution of 1% (w/v) XG. These values are in the same order of magnitude as determined for other published formulations of particulate media, which were demonstrated to support the printing of materials with a wide range of viscosities [13, 14, 16]. Hybrids made of 1% (w/v) XG solution and alginate particles, mixed in different ratios, presented with similar rheological properties as its components. On the other hand, supplementing the particulate alginate with pure culture media resulted in a significantly reduced viscosity (Figure 2g, h).

3D printing of accurate constructs relies on the capacity to extrude the material and preserve its structure to reliably reflect the geometry depicted by the digital data. We noticed that while printing in particulate alginate support medium or even in pure, 1% XG solution is feasible (Figure 3a,b), the hybrid support, which contains as low as 0.05% (w/v) XG, allowed fabrication with a superior shape fidelity. The NPCH was deposited in this medium as aligned cylindrical strands with straight contour (Figure 3c,d), showing cross-section of high circularity value (Figure 3e-g). It is worth mentioning that the supported NPCH printouts retain their shape over long time periods, even without being subjected to a final thermal curing. This was clearly demonstrated previously by our group, when a small-scale human heart was printed in a cooled environment in a several-hours-long fabrication process. Upon curing and extraction, the construct maintained an undistorted, intact structure[21]. In contrast to NPCH, other biomaterials may diffuse or intermix with the support medium over time. This can be overcome by adapting the formulation of the hybrid support medium to include specific agents that will cure the biomaterials promptly upon their extrusion.

Printing large, volumetric structures may be a long process in which both the bioinks and the supporting medium are required to maintain their physical properties in order for the printout to be uniform and accurate. However, over time, aggregation of the particles composing the support medium may impair printing quality. Thus, we next sought to test the ability of the media to maintain their supporting qualities over time. The media were vigorously vortexed to disassemble aggregates, centrifuged to remove air bubbles and incubated at room temperature for 3 minutes, 3 hours and 18 hours before printing. After 3 minutes, the printed strands in both the particulate alginate and the hybrid medium showed a straight filament morphology. Still, the hybrid medium supported printing of strands with smoother contour. After 3 hours, the strands printed within the particulate alginate appeared blurry and inconsistent, as opposed to the hybrid support, which maintained the alignment and accuracy of the printed strands even after 18 hours (Figure 4 a,b). This phenomenon was also evident when examining the printing process from a side view (Figure 4c, Sup video 1 and 2). Such a viewpoint also allowed to follow the process in which adjacent printed layers gradually fuse (Figure 4d), a prerequisite for attaining an intact, stable structure upon curing and extraction from the support.

The ability to precisely print bioinks at a micron-scale high resolution is a perquisite for engineering anatomically relevant living structures. For example, the diameter of renal tubules and blood capillaries ranges between 20-40 and 5-10 micrometers, respectively[24–26]. Here, we have demonstrated the ability to print NPCH into the hybrid support medium using the smallest inner-diameter needles that are disposable, mass-produced and commercially-available (34G; 80 μm I.D). By applying different printing speeds (feed rates; FR), filaments with diameters ranging between 60 to 20 μm were successfully printed (Figure 5a-c). Printing of filaments with smaller diameters of down to 10 μm (9.97±1.86 μm) could also be achieved using custom-made, pulled glass pipettes (Figure d,e). Smaller diameter filaments can be attained by using pipettes with smaller inner diameters. However, these are not relevant for cell printing as most cell sizes exceed this diameter, and a high shear stress may rapture them.

To demonstrate the ability to print living cells, NIH/3T3 fibroblasts were mixed with NPCH and printed as grid-like structures in the hybrid support medium. After curing at 37°C for 30 minutes, the support medium was extracted by treatment with alginate lyase that destabilized the alginate particles, leaving the structures floating in the medium (Figure 5f). Cell viability was then evaluated immediately and 24 hours post-extraction, confirming that the whole process was nondestructive to the incorporated cells (Figure 5 g,h). To further prove the biocompatibility of the system, primary endothelial and cardiac cells were used to assess the effect of a direct-exposure to the hybrid support and to its degradation products. Although cells encapsulated inside NPCH are not directly exposed to the calcium-crosslinked alginate particles, such a temporal contact did not cause an acute toxicity (Sup figure 1a). Also, no toxic effect was evident after a prolonged exposure to the soluble elements of the system, i.e., XG, alginate lyase and alginate degradation products (Sup figure 1b). Finally, we sought to demonstrate the potential of this method to support accurate printing of complex anatomical structures at high resolution. To this end, we used two NPCH-loaded printheads to fabricate the structures of both the parenchyma and the major blood vessels in a cross-section of a small-scale human heart (Figure 5i).

Summary and Conclusions

In this work, we provide a deep level of insight into our previously presented new concept of printing in a hybrid support medium[21]. This hybrid, based on a combination of particulate crosslinked hydrogel and an additional soluble polymer, can be used to provide an appropriate support for 3D printing of soft biomaterials. Specifically, we chose to characterize and demonstrate the competency of a unique formulation, comprised of calcium-crosslinked alginate nanoparticles and xanthan gum. This preparation presents superb qualities, allowing long-term high resolution and accurate printing of bio-structures with high degree of anatomical complexity. While various soluble polymers and thickening agents such as methylcellulose, agarose and glycerol were evaluated as additives to improve the printing-supporting capability of the alginate particulate medium, we found xanthan gum to give the best overall results. Notably, the addition of carboxymethyl cellulose (CMC), that like xanthan is a negatively-charged gum with a cellulose backbone, also improved long-term printing accuracy. Nevertheless, it resulted in inferior printing fidelity when compared to XG at similar ranges of concentrations and viscosities (Sup figure 2). While the reason for the superiority of XG addition in terms of printing-supporting capability is yet to be elucidated, the latter is known for its unique rheological properties. Its shear thinning behavior, high viscosity at low concentrations and durability to extreme conditions make it a commonly used stabilizer and viscosity modifier in numerous industrial and research applications [27–30]. It is also known that mixing XG with alginate solutions results in a strand-like phase separation [31, 32]. This phenomenon could be attributed to distinct features of the XG molecule, like its length, charge distribution, branched structure and stiffness that may affect its spatial arrangement and interaction with anionic polymers. It is possible that the observed impact of XG on the micro-composition of the particulate medium and its printing supporting qualities results from a “lubrication-like effect”. The XG molecules may orient in-between the alginate particles, prevent them from aggregating and allow them to smoothly slide over each other when the needle is traversing.

The alginate-XG hybrid medium described herein is cell friendly and stable at a wide range of temperatures relevant for bioengineering applications. It has been tested and verified to preserve its qualities when chilled, at ambient temperature or when heated to 37°C, indicating on its capacity to support printing of diverse bioinks with different thermal behaviors. We have demonstrated the excellent capacity of this formulation to support printing of complex structures made of thermally curable NPCH, which can be prepared from autologous materials and loaded with the patient’s own cells[19–21]. Another feature that distinguishes this hybrid medium is its high transparency. This quality greatly facilitates on–line monitoring of the printing and may improve the efficiency of any related process that requires light permeability. Finally, the fact that the support medium can be extracted by non-toxic, delicate procedures is highly important when handling soft and fragile printed bio-structures that may contain living cells.

Overall, we believe that such hybrid support media could be of a great added value for 3D printing of soft biomaterials, without compromising on biocompatibility, long-term accuracy, printing resolution, transparency and ease of extraction.

Methods

Xanthan gum pre-treatment

Before being used as a support medium supplement, xanthan gum (XG) was sterilized and treated to deactivate endotoxins. Briefly, XG (XANTURAL 180, kindly provided by CP Kelco) was dissolved in double distilled water (DDW) containing 150mM sodium chloride, to reach a 4% (w/v) viscous solution. Following autoclaving, the preparation was supplemented with 5M NaOH solution at 4:1 volume ratio and mixed thoroughly to achieve a homogenous mixture containing 1M NaOH. After incubation for 24h at RT, the mixture was transferred to a large sterile syringe and extruded into a perforated vessel soaked in a constantly stirred solution of 50% (v/v) ethanol that is 10 times larger in volume. Under these conditions, the XG remained insoluble while the ions contributed by the NaCl and NaOH diffuse into the surrounding liquid. The 50% ethanol solution was changed daily until its pH reached neutrality, after which it was replaced with a 70% (v/v) ethanol solution. When the pH of the solution remained stable between exchanges (reaching a value that resembles that of a naïve 70% ethanol solution), the XG is removed from the solution and dried under a jet of a sterile air. Residual water and ethanol molecules were then removed under a deep vacuum.

Support medium preparation—For the generation of the printing support medium, an aqueous solution containing 0.32% (w/v) sodium alginate (PROTANAL LF 200 FTS, a generous gift from FMC BioPolymer), 0.25% (w/v) pre-treated xanthan gum, 37.5mM sodium chloride and 9.56mM calcium carbonate (as suspension, Sigma-Aldrich) was prepared. While constantly stirred, the mixture was supplemented with freshly prepared, pre–dissolved D-(+)-Gluconic acid δ-lactone (Sigma-Aldrich) to reach a final concentration of 19.15mM. This results in a slow decrease in the pH, gradual solubilization of the calcium carbonate and liberation of the calcium ion that crosslinks the alginate. When the solution's viscosity is increased to a level that prevents precipitation of the calcium carbonate, the stirring was stopped and the mixture was incubated at RT for 24h. Double distilled water at 4 times the volume of the resulted hydrogel were then added, followed by homogenization at 25,000 RPM for 2 minutes (HOG-020 homogenizer with GEN-2000 generator probe, MRC ltd, Israel). The homogenate was incubated for 24h at 4°C, and then centrifuged at 15,800g for 20 min. The pellet was washed by resuspention (vigorous vortexing) in double distilled water, recentrifuged, resuspended in DMEM/F12 (HAM) 1:1 culture media (Biological Industries, Israel) and centrifuged again, after which the supernatant was discarded. Next, 1% (w/v) xanthan gum in DMEM/F12 (HAM) 1:1 media was added to the pellet at 1:20 volume ratio (or other, as indicated) to reach a final concentration of ~0.05% (w/v), followed by vigorous vortexing to homogenize the mixture. The mixture was then incubated for 3-4 or 6-8 days at RT or 4°C, respectively, and vigorously vortexed daily. After this period, the mixture could be used immediately to support printing, or, alternatively, be stored at RT or 4°C for later use.

For the generation of particulate support medium supplemented with carboxymethylcellulose (CMC), the same preparation procedure was performed, using

sodium carboxymethylcellulose (ultra-high viscosity, Sigma-Aldrich) instead of XG, at the same concentrations as indicated.

To demonstrate the transparency of alginate hydrogel crosslinked by internal gelation (fig 1a), the alginate gel was prepared as described above, excluding XG supplementation. External gelation was performed by crosslinking sodium alginate using 1% (w/v) CaCl2 solution.

Printable biomaterials preparation—Neutral, pepsinized collagen-based hydrogels (NPCH) were prepared as previously described [21]. Alternatively, PureCol® EZ Gel type I bovine collagen solution (neutral, pepsin treated; Advanced BioMatrix) was used for printing. To improve visualization, when indicated, printing materials were supplemented with 1 μm blue (fluorescent when exited at ~620 nm) or red polystyrene microparticles (Sigma-Aldrich) or with lipid nanoparticles encapsulating Cy3 or Cy5 molecules (a kind gift from Prof. Dan Peer, Tel Aviv University). For generation of a cell-containing bioink, NIH/3T3 mouse fibroblasts were mixed with NPCH to a final concentration of 5×10^6 cells ml^{-1}.

Printing in support media—Support media were vortexed vigorously, briefly centrifuged to remove air bubbles and transferred into a transparent, open sterile plastic box. Printing was performed within one hour from vortexing, unless indicated otherwise. Constructs were printed using 3DDiscovery® printer (regenHU, Villaz-Saint-Pierre, Switzerland) by extrusion (through 30G needles, unless stated otherwise) according to designs generated by BioCAD™ drawing software (regenHU) or according to data from STL files (sliced and processed by BioCAM™ software (regenHU)) which were downloaded from Thingiverse (www.thingiverse.com “Anatomical Human Heart” by 517860 (modified), under the Creative Commons - Attribution - Share Alike license - CC BY-SA 3.0 https://creativecommons.org/licenses/by-sa/3.0/). Printouts were visualized by an inverted fluorescence microscope (Nikon Eclipse TI) or an upright confocal microscope (Nikon ECLIPSE NI-E). The printing process was captured from a side-view using a long working distance Dino-Light digital microscopes (AnMo Electronics, Taiwan). For extraction of the printed structures from the support medium, the box was incubated at 37°C for 30 min to cure the bioink. Then, the support medium was supplemented with alginate lyase (Sigma-Aldrich, 1U/ml) and incubated at 37°C. The digested support medium was gradually aspirated and replaced with growth medium.

Rheological properties—Rheological measurements (n=3) were taken using Discovery HR-3 hybrid Rheometer (TA Instruments, DE) with 8 mm diameter parallel plate geometry with a Peltier plate to maintain the sample temperature at 21°C. Stress sweeps where done by applying a fixed frequency of 1Hz. Frequency sweeps where performed by applying a strain of 1%.

Microscopic examination of support media—Samples of particulate alginate and hybrid support media were diluted 1:4 (v/v) in cell medium or water; or in cell medium or water containing 0.05% (w/v) XG, respectively. For environmental scanning electron microscopy (ESEM), diluted samples (in water) of hybrid support medium were observed

under Quanta 200 FEG (ThermoFisher scientific, Waltham, US) using ESEM mode (<26 mbar). For light microscopy examination, diluted samples (in cell medium) of particulate alginate or hybrid support media were visualized by inverted light microscope (Nikon Eclipse TI).

Cell culture—NIH/3T3 cells (ATCC) were maintained in Dulbecco's modified Eagle medium (DMEM) supplemented with 10% fetal bovine serum (FBS), 1% Glutamine and 1% penicillin/streptomycin (Biological Industries). Primary human umbilical vein endothelial cells (HUVECs, Angio-Proteomie) were maintained in EGM-2 (Lonza, Basel, Switzerland) supplemented as according to the manufacturer instructions. Neonatal cardiac cells were isolated according to Tel Aviv University ethical use protocols from intact ventricles of 1- to 3-day-old neonatal Sprague-Dawley rats. Cells were isolated using 6 cycles (37 °C, 30 min each) of enzyme digestion with collagenase type II (95 U mL^{-1}, Worthington, Lakewood, New Jersey) and pancreatin (0.6 mg mL^{-1}, Sigma-Aldrich) in DMEM. After each round of digestion, cells were centrifuged (600 g, 5 min) and resuspended in M-199 culture medium (Biological Industries) supplemented with 0.6×10^{-3} M CuSO4 · 5H2O, 0.5×10^{-3} M ZnSO4 · 7H2O, 1.5×10^{-3} M vitamin B12 (Sigma-Aldrich), 500 U mL^{-1} penicillin, 100 mg mL-1 streptomycin and 0.5% FBS. After the isolation procedure, cells were cultured in M-199 medium with 5% FBS and supplements as indicated above. Cell number was determined by a hemocytometer and trypan blue exclusion assay. Cells were cultured under a humidified atmosphere at 37°C with 5% CO2.

Viability assay—Viability of NIH/3T3 cells in NPCH printed constructs was determined using a live/dead fluorescent staining with fluorescein diacetate (Sigma-Aldrich, 7 μg/mL) and propidium Iodide (Sigma-Aldrich, 5 μg/mL) for 30 min at 37°C. Cells were visualized by inverted fluorescence microscope (Nikon Eclipse TI) and the number of live and dead cells was determined by manual counting using NIS Elements software (Nikon) from at least 3 different microscopic fields ($n \geq 3$ in each experiment). Primary endothelial and cardiac cells were used to assess the effect of a direct-exposure to the hybrid support and its degradation products. Primary human umbilical vein endothelial cells (HUVEC) were seeded at a density of 2.5 x 10^4 cells per well in 96-well plates. Four hours later, the cells were exposed to the hybrid support medium (diluted 1:4 v/v in growth medium) for 5 h. Microscopic images were taken using inverted microscope (Nikon Eclipse TI) at the end of the treatment. The cells were then cultured in fresh growth medium for 24 h, and tested for viability using PrestoBlue™ assay (Invitrogen, USA), with fluorescence reading taken with Infinite M200 PRO Microplate reader (Tecan, Switzerland). Primary neonatal rat cardiac cells were seeded at a density of 1 x 10^4 cells per well in 96-well plates. Seventy–two hours later, cells were exposed to hybrid support medium that has been diluted at a ratio of 1:4 v/v in growth medium and digested with alginate lyase (Sigma-Aldrich, 10 U/ml) for 1 h at 37°C. The mixture was passed through 0.22-micron mesh before being administrated to the cells to filter out non–soluble components. After 24 h, microscopic images were taken using inverted microscope (Nikon Eclipse TI) and the medium was changed to fresh growth medium. After 6 h, the cells were tested for viability using PrestoBlue™ assay with fluorescence reading taken with Infinite M200 PRO Microplate reader. All values were

normalized to the control groups, consisted of cells treated with non-supplemented growth medium (n≥3).

Statistical and Image Analysis—Statistical data are presented as means ± s.d. Differences between samples were assessed by student's t-test. $p < 0.05$ was considered significant. "ns" denotes not significant. Analyses were performed using GraphPad prism version 6.00 for windows (GraphPad Software). Images were analyzed using ImageJ (NIH).

Supplementary Material

Refer to Web version on PubMed Central for supplementary material.

Acknowledgements

T.D. received support from European Research Council Starting Grant 637943, the Israeli Science Foundation (700/13), the Israel Ministry of Science, Technology and Space (3-12587) and Moxie Foundation.

References

1. Dvir T, Timko BP, Kohane DS, Langer R. Nanotechnological strategies for engineering complex tissues. Nature Nanotechnology. 2011; 6:13–22.
2. Fleischer S, Miller J, Hurowitz H, Shapira A, Dvir T. Effect of fiber diameter on the assembly of functional 3D cardiac patches. Nanotechnology. 2015; 26 291002 [PubMed: 26133998]
3. Shapira A, Feiner R, Dvir T. Composite biomaterial scaffolds for cardiac tissue engineering. International Materials Reviews. 2016; 61:1–19.
4. Murphy SV, Atala A. 3D bioprinting of tissues and organs. Nature biotechnology. 2014; 32:773.
5. Shapira A, Noor N, Asulin M, Dvir T. Stabilization strategies in extrusion-based 3D bioprinting for tissue engineering. Applied Physics Reviews. 2018; 5 041112
6. Mandrycky C, Wang Z, Kim K, Kim D-H. 3D bioprinting for engineering complex tissues. Biotechnology Advances. 2016; 34:422–434. [PubMed: 26724184]
7. Zhang YS, Oklu R, Dokmeci MR, Khademhosseini A. Three-Dimensional Bioprinting Strategies for Tissue Engineering. Cold Spring Harbor perspectives in medicine. 2018; 8 a025718 [PubMed: 28289247]
8. Jungst T, Smolan W, Schacht K, Scheibel T, Groll J. Strategies and Molecular Design Criteria for 3D Printable Hydrogels. Chemical Reviews. 2016; 116:1496–1539. [PubMed: 26492834]
9. Kelly BE, et al. Volumetric additive manufacturing via tomographic reconstruction. Science. 2019; 363:1075–1079. [PubMed: 30705152]
10. Grigoryan B, et al. Multivascular networks and functional intravascular topologies within biocompatible hydrogels. Science. 2019; 364:458–464. [PubMed: 31048486]
11. Hölzl K, et al. Bioink properties before, during and after 3D bioprinting. Biofabrication. 2016; 8 032002 [PubMed: 27658612]
12. Hinton TJ, et al. Three-dimensional printing of complex biological structures by freeform reversible embedding of suspended hydrogels. Science advances. 2015; 1 e1500758 [PubMed: 26601312]
13. Bhattacharjee T, et al. Writing in the granular gel medium. Science advances. 2015; 1 e1500655 [PubMed: 26601274]
14. Jin Y, Compaan A, Chai W, Huang Y. Functional Nanoclay Suspension for Printing-Then-Solidification of Liquid Materials. ACS Applied Materials & Interfaces. 2017; 9:20057–20066. [PubMed: 28534614]
15. Jin Y, Chai W, Huang Y. Printability study of hydrogel solution extrusion in nanoclay yield-stress bath during printing-then-gelation biofabrication. Materials Science and Engineering: C. 2017; 80:313–325. [PubMed: 28866170]

16. Skylar-Scott MA, et al. Biomanufacturing of organ-specific tissues with high cellular density and embedded vascular channels. Science Advances. 2019; 5 eaaw2459 [PubMed: 31523707]
17. Lee A, et al. 3D bioprinting of collagen to rebuild components of the human heart. Science. 2019; 365:482–487. [PubMed: 31371612]
18. Antoine EE, Vlachos PP, Rylander MN. Review of collagen I hydrogels for bioengineered tissue microenvironments: characterization of mechanics, structure, and transport. Tissue engineering Part B, Reviews. 2014; 20:683–696. [PubMed: 24923709]
19. Shevach M, et al. Omentum ECM-based hydrogel as a platform for cardiac cell delivery. Biomedical Materials. 2015; 10 034106 [PubMed: 25970726]
20. Edri R, et al. Personalized Hydrogels for Engineering Diverse Fully Autologous Tissue Implants. Advanced Materials. 2018 1803895
21. Noor N, et al. 3D Printing of Personalized Thick and Perfusable Cardiac Patches and Hearts. Advanced Science. 2019; 6 1900344 [PubMed: 31179230]
22. Kuo CK, Ma PX. Ionically crosslinked alginate hydrogels as scaffolds for tissue engineering: Part 1. Structure, gelation rate and mechanical properties. Biomaterials. 2001; 22:511–521. [PubMed: 11219714]
23. Ingar Draget K, Østgaard K, Smidsrød O. Homogeneous alginate gels: A technical approach. Carbohydrate Polymers. 1990; 14:159–178.
24. Li Q, et al. Automated quantification of microstructural dimensions of the human kidney using optical coherence tomography (OCT). Opt Express. 2009; 17:16000–16016. [PubMed: 19724599]
25. Müller B, Fischer J, Dietz U, Thurner PJ, Beckmann F. Blood vessel staining in the myocardium for 3D visualization down to the smallest capillaries. Nuclear Instruments and Methods in Physics Research Section B: Beam Interactions with Materials and Atoms. 2006; 246:254–261.
26. Müller, B, , et al. High-resolution tomographic imaging of microvessels. Vol. 7078. SPIE; 2008.
27. Kumar A, Rao KM, Han SS. Application of xanthan gum as polysaccharide in tissue engineering: A review. Carbohydrate Polymers. 2018; 180:128–144. [PubMed: 29103488]
28. Habibi H, Khosravi-Darani K. Effective variables on production and structure of xanthan gum and its food applications: A review. Biocatalysis and Agricultural Biotechnology. 2017; 10:130–140.
29. Petri DFS. Xanthan gum: A versatile biopolymer for biomedical and technological applications. Journal of Applied Polymer Science. 2015; 132
30. Tan E, Yeong WY. Direct Bioprinting of Alginate-Based Tubular Constructs Using Multi-Nozzle Extrusion-Based Technique. 2014
31. Boyd MJ, et al. Strand-like phase separation in mixtures of xanthan gum with anionic polyelectrolytes. Food Hydrocolloids. 2009; 23:2458–2467.
32. Boyd, MJ, , et al. Gums and Stabilisers for the Food Industry. Vol. 12. The Royal Society of Chemistry; 2004. 262–271.

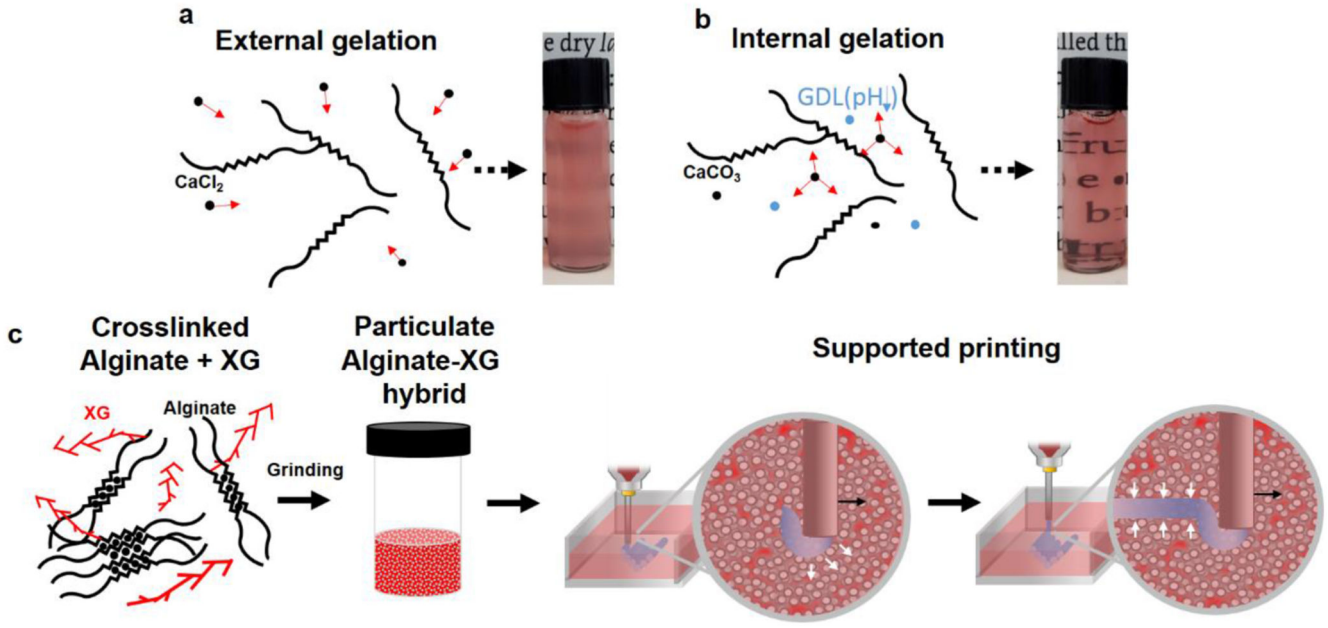

Figure 1. Concept schematic.

a. External and **b.** Internal gelation of alginate resulted in hydrogels that differ in their homogeneity and opacity. In the external gelation method, the alginate is non-homogenously crosslinked by diffusion of externally-introduced ions. In the internal gelation strategy, the crosslinking ion (such as Ca^{2+}) is slowly liberated from a pre-mixed insoluble salt (such as $CaCO_3$) upon acidification of the medium, resulting in homogenously crosslinked gels **c.** Preparation of the hybrid support medium for 3D printing. XG-supplemented alginate is slowly crosslinked by internal gelation and grinded to form a particulate hybrid medium. The latter is locally fluidized around the traversing needle and rapidly reorganizes to embrace and stabilize the printed strand.

Europe PMC Funders Author Manuscripts

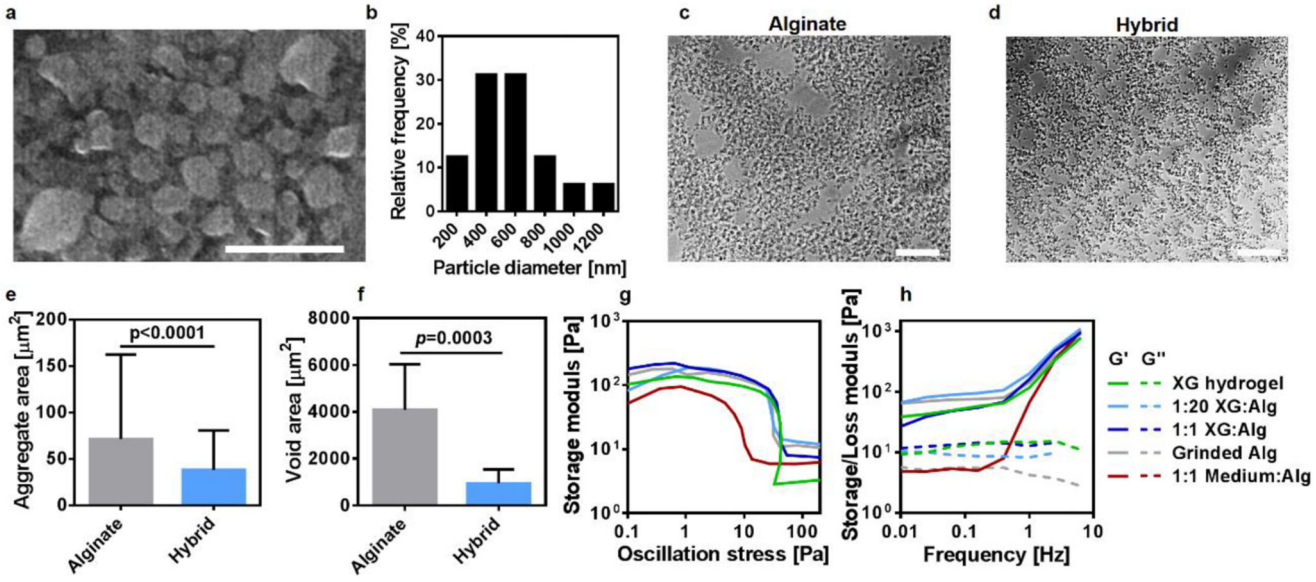

Figure 2. Support medium characterization.

a. An ESEM image of the alginate nanoparticles in a diluted support medium and **b.** A histogram of particle diameter. Light microscopy images showed that the addition of XG (to a final concentration of 0.05% w/v) resulted in homogenously distributed smaller aggregates (**c** and **d**). This could be quantitatively presented by **e.** Average aggregate area and **f.** Average void area between aggregates. The rheological properties of the different combinations (represented as volume ratios) between alginate particles, 1% w/v XG solution and pure culture media were evaluated by **g.** Stress and **h.** Frequency tests, indicating on their yield stress and viscoelastic features. Scale bars: (a) = 2 μm, (c),(d) = 100 μm.

Europe PMC Funders Author Manuscripts

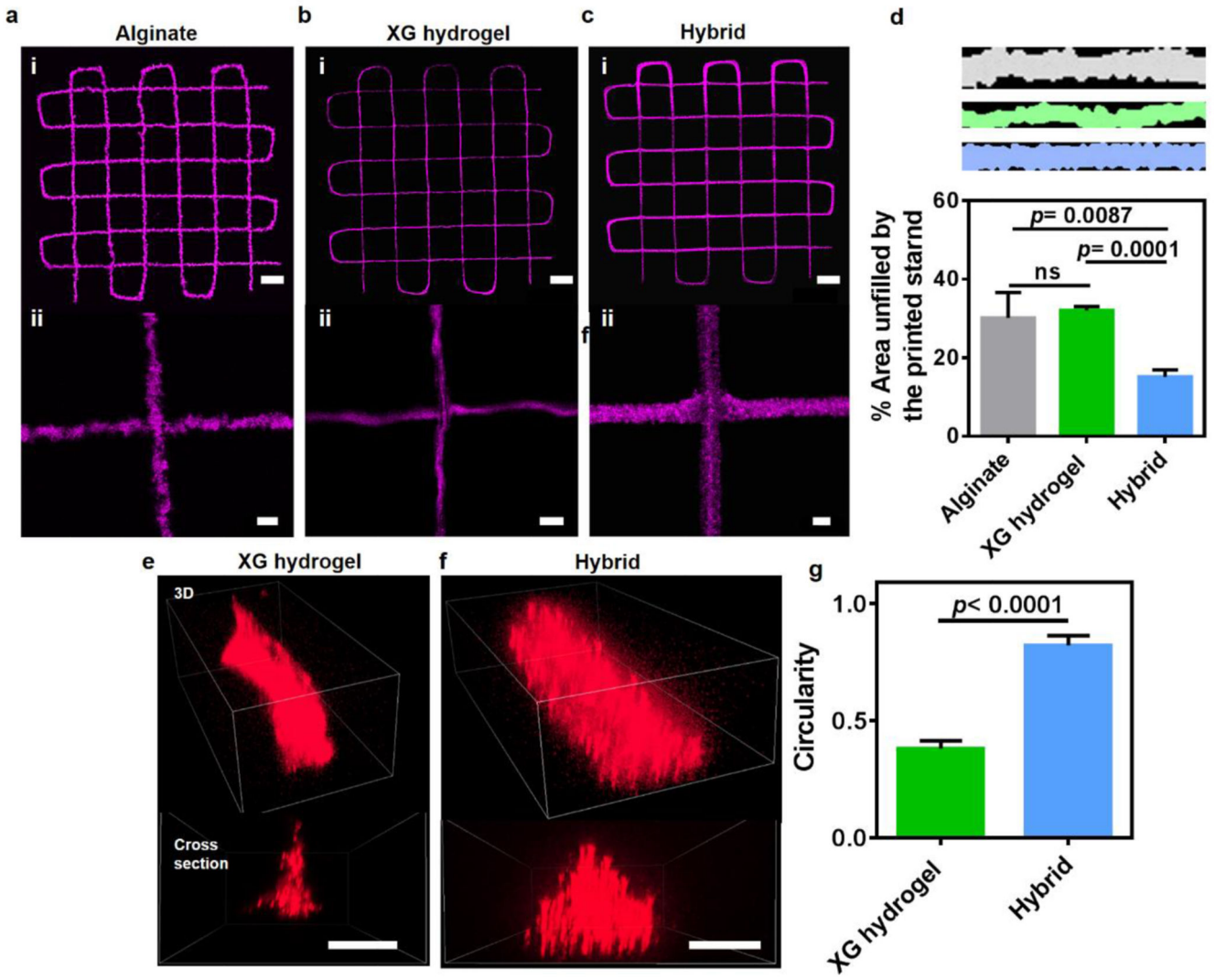

Figure 3. Shape fidelity of structures printed with NPCH in support media.

Images of fluorescent microparticle-loaded NPCH printed in **a.** Particulate alginate **b.** Pure 1% XG solution and **c.** Hybrid support medium containing 0.05% (w/v) XG. **d.** A quantitative comparison between the printing-supporting qualities of each medium. Evaluation was performed by delineating the printed strands from top-view with the best fitted rectangle, and calculating the unoccupied area. Lower values represent higher shape fidelity. **e-f.** Confocal 3D reconstruction of fluorescent nanoparticles-loaded NPCH strands printed in **e.** Pure 1% XG solution and **f.** Hybrid support medium. **g.** Quantification of the strands' cross section circularity (=$4\pi\times$(Area/Perimiter^2)). Scale bars: (a), (b), (c): i = 1 mm, ii = 100 μm. (e), (f) = 50 μm.

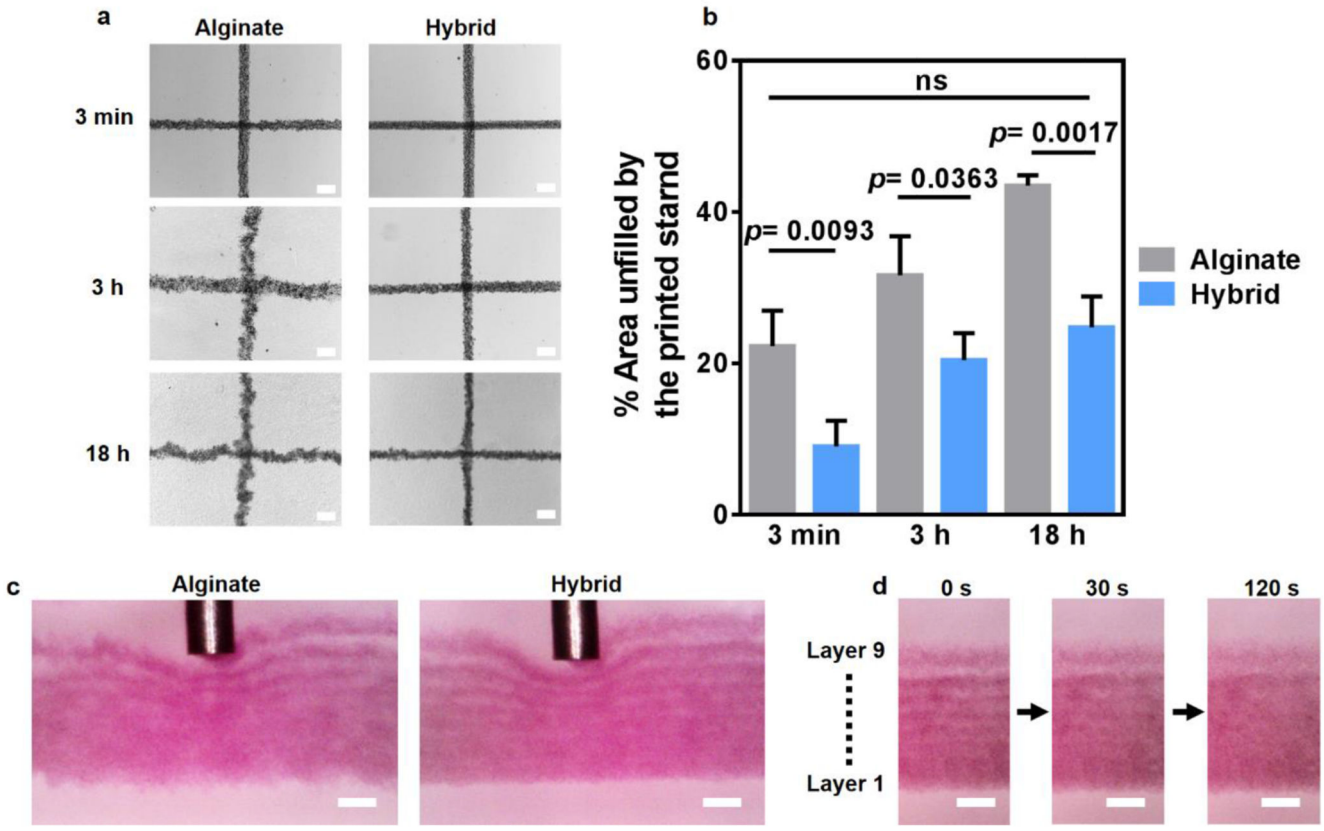

Figure 4. The effect of time on printing-supporting qualities of different media.

a. Top-view images of microparticle-loaded NPCH strands printed at different time points following vortexing of the support media. **b.** A quantitative comparison between the printing-supporting qualities of each medium over time. Evaluation was performed by delineating the printed strands from top-view with the best fitted rectangle and calculating the unoccupied area. Lower values represent higher shape fidelity. **c.** Microscopic side views of printed microparticle-loaded NPCH strands within support media, 18 hours after vortex. **d.** Fusion of printed NPCH layers into a continues structure within the hybrid support medium. The ninth, upper layer was printed 180 s after the first, bottom layer. The multilayered construct was then visualized following 0, 30 and 120 s post-printing. Scale bars: (a), (c) and (d) = 200 μm.

Europe PMC Funders Author Manuscripts

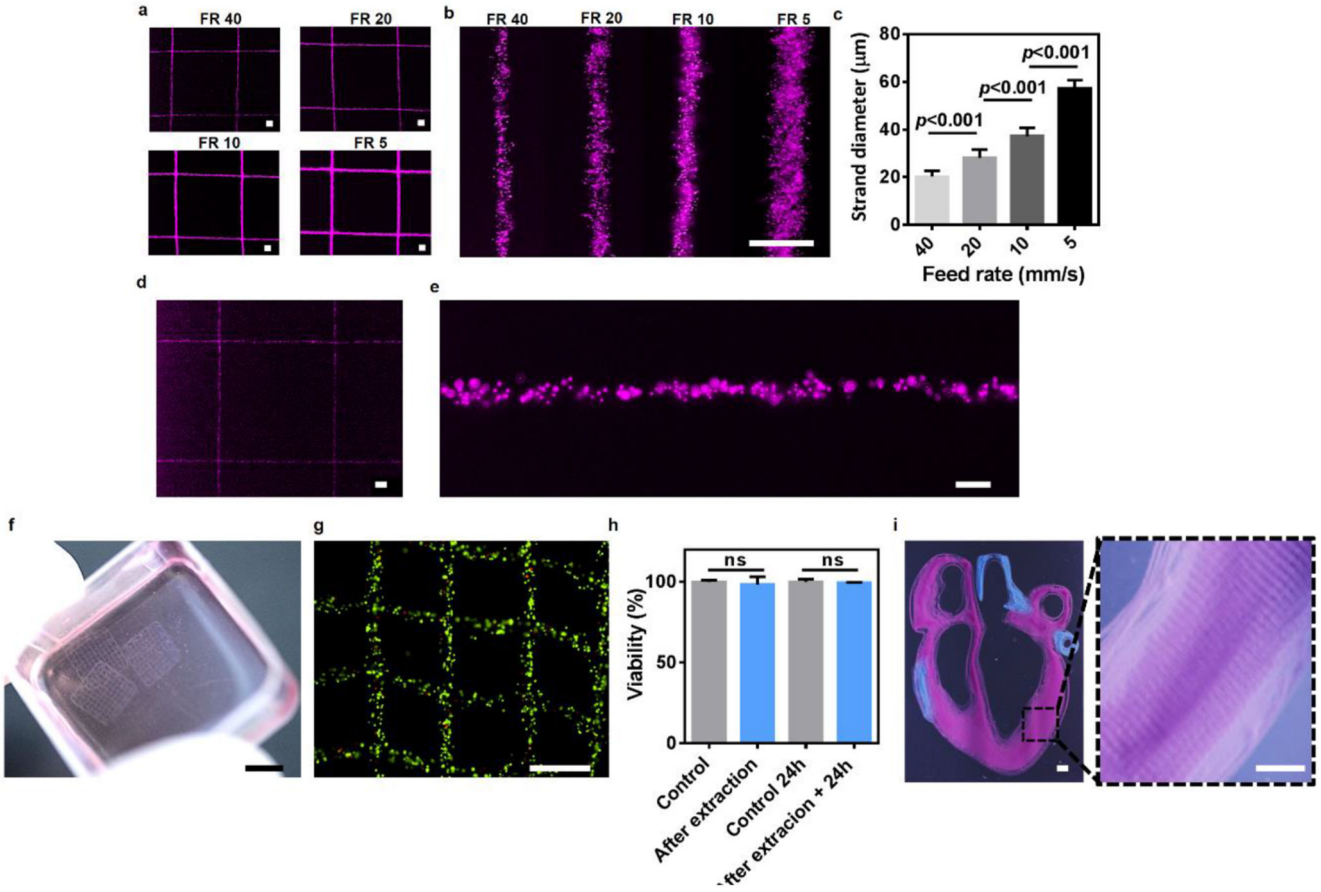

Figure 5. High resolution printing of NPCH in hybrid support medium.

a. Low and **b**. High magnification images of fluorescent microparticle-incorporating NPCH printed in different feed rates (FR, mm/s) using 34G needle and **c.** the diameter of the printed filaments. **d.** Low and **e.** High magnification images of 10 μm diameter fluorescent microparticle-loaded NPCH strands printed using a pulled glass pipette. **f.** A macroscopic view of fibroblasts-laden NPCH printed structures after extraction from the support medium and **g.** A microscopic image of their live (green)/dead (red) staining following cultivation for 24 hours. **H**. Cell viability in the printed structures immediately after extraction and following cultivation for 24 hours. Cell-containing NPCH bioink, casted into culture dishes, served as a control. **i.** Macroscopic and **inset.** Microscopic images showing a high resolution printing of a cross-section of a small-scale human heart. Two distinct printheads loaded with microparticle-containing NPCH were used to print both parenchymal tissue (purple) and major blood vessels (blue). Scale bars: (a), (b), (d) = 100 μm. (e) = 20 μm. (f)= 5 mm. (g)= 500 μm. (i), inset = 1 mm.

Europe PMC Funders Author Manuscripts